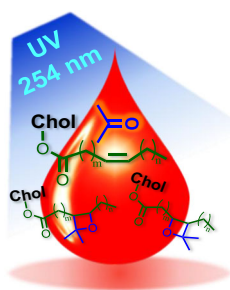


# Uncovering Structural Diversity of Unsaturated Fatty Acyls in Cholesteryl Esters via Photochemical Reaction and Tandem Mass Spectrometry

Jia Ren, Elissia T. Franklin, Yu Xia

Department of Chemistry, Purdue University, West Lafayette, IN 47907-2084, USA



**Abstract.** Mass spectrometry analysis of cholesteryl esters (CEs) faces several challenges, with one of them being the determination of the carbon–carbon double bond (C=C) locations within unsaturated fatty acyl chains. Paternò-Büchi (PB) reaction, a photochemical reaction based on the addition of acetone to C=C, is capable of C=C location determination when coupled with tandem mass spectrometry (MS/MS). In this study, the PB reaction conditions were tailored for CEs and subsequent nano-electrospray ionization (nanoESI). A solvent system containing acetone/methanol/dichloromethane/water (40/30/20/10, volume ratios) and 100  $\mu\text{M}$  LiOH was determined to be optimal, resulting in reasonable PB reaction yield (~30%) and good ionization efficiency (forming lithium adduct of CEs). Collision-induced dissociation

(CID) of the PB reaction products produced characteristic fragment ions of CE together with those modified by the PB reactions, such as lithiated fatty acyl ( $[\text{FA} + \text{Li}]^+$ ) and its PB product ( $[\text{FA} - \text{PB} + \text{Li}]^+$ ).  $\text{MS}^3$  CID of  $[\text{FA} - \text{PB} + \text{Li}]^+$  led to abundant C=C diagnostic ion formation, which was used for C=C location determination and isomer quantitation. A PB- $\text{MS}^3$  CID approach was developed and applied for CE analysis from human plasma. A series of unsaturated CEs was identified with specific C=C locations within fatty acyl chains. Absolute quantitation for each CE species was achieved including coexisting C=C location isomers, such as  $\Delta 9$  and  $\Delta 11$  isomers of CE 18:1 and  $\omega$ -6 and  $\omega$ -3 isomers of CE 18:3. These results show that PB-MS/MS is useful in uncovering structural diversity of CEs due to unsaturation in fatty acyls, which is often undetected from current lipid analysis approach. **Keywords:** C=C determination, Cholesteryl esters, Paternò-Büchi reaction, Lipidomics, Tandem mass spectrometry

Received: 29 January 2017/Revised: 22 February 2017/Accepted: 24 February 2017/Published Online: 17 April 2017

## Introduction

In all types of cells, the balance between the biologically active free sterols and the inactive storage form as sterol esters, viz. sterol homeostasis, is important [1, 2]. Cholesterol esters (CEs) have long fatty acid chains attached to the 3-hydroxyl group of cholesterol (Figure 1) and function as a biologically inert storage form of cholesterol [3]. They are less polar than free cholesterol; therefore, they are a preferred form within lipoprotein particles for transportation. CEs are bio-

synthesized in two different pathways. One relies on acyl-CoA cholesterol acyltransferase (ACAT) to esterify sterols inside the cell [4, 5]. The other one occurs in the extracellular space (i.e., bloodstream), catalyzed by lecithin cholesterol acyl transferase (LCAT) [6]. In this process, fatty acyls at *sn*-2 position of phosphatidylcholines are transferred to cholesterol and produce CEs. Plasma CE concentrations can be as high as 1–3  $\text{mmol L}^{-1}$ , and they tend to contain relatively high proportions of polyunsaturated fatty acyl (PUFA) chains [7]. Recent studies show that LCAT also serves in reverse cholesterol transport and polyunsaturated CE synthesis, whereas, ACAT2 [8] (one isoform of ACAT) promotes accumulation of mono-unsaturated and saturated CE in lipoprotein particles containing apolipoprotein B [9]. Given the importance of cholesterol homeostasis for normal functions of cells, abnormal CE levels are often linked with various pathological conditions, including

**Electronic supplementary material** The online version of this article (doi:10.1007/s13361-017-1639-6) contains supplementary material, which is available to authorized users.

Correspondence to: Yu Xia; e-mail: yxia@purdue.edu

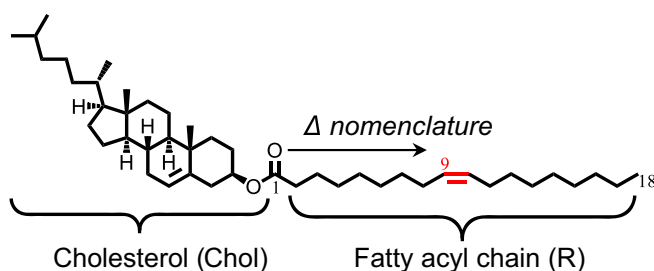


**Figure 1.** Nomenclature of cholesteryl ester. The C=C double bond is indicated as cis- $\Delta^9$  in  $\Delta^x$  nomenclature system for CE 18:1 (9Z)

metabolic disorders [10], heart disease [11], and cancer [12, 13]. CE profiling, a subset study of metabolomics and lipidomics, has been frequently used as a means to discover biomarkers for disease monitoring or diagnosis [14].

Mass spectrometry (MS)-based lipid analysis has been established as a powerful tool for the identification and quantitation of a variety of lipid classes from biological matrixes, offering a combined advantage of high sensitivity, speed, and detailed structural information [15]. Many different MS techniques have been applied to CE analysis with both successes and limitations. Conventionally, the fatty acyl composition of CE is analyzed by gas chromatography (GC)-MS via electron ionization (EI) or chemical ionization (CI). Because of limited volatility, CEs need to be hydrolyzed and the methylated fatty acyls are subjected to GC-MS, the process of which requires relatively long analysis time (in hours) [16]. The development of electrospray ionization (ESI) [17] has greatly expanded the spectrum of lipids that can be analyzed by MS. Han and Gross were amongst the first to recognize the potential of ESI-MS for global lipid analysis from biological systems [18]. Soon thereafter, two techniques based on ESI-MS were established as the main methods for current lipidomics studies: shotgun lipid analysis of crude lipid extract [19, 20] and ESI-MS coupled with liquid chromatography (LC) separations [21, 22].

Given the nonpolar nature of CE, adduct ion formation is employed to enhance ionization efficiency of CE in ESI, with  $\text{NH}_4^+$ ,  $\text{Li}^+$ , and  $\text{Na}^+$  being frequently used as adduct ions for positive ion mode. Tandem mass spectrometry (MS/MS) via low energy collision-induced dissociation (CID) of CE adduct ions has been developed for the identification and quantitation of CEs from mixtures [23]. For instance, CID of the ammonium adduct of CE generates a dominant fragment ion at  $m/z$  369 (cholestene cation), allowing the use of product ion scan (PIS) for quantitation of CEs from lipid mixtures [24]. Collisional activation of lithiated or sodiated CE ions results in an abundant neutral loss of cholestere (368 Da) and forms  $\text{Li}^+$  or  $\text{Na}^+$  adduct of fatty acyl ions [25, 26]. This fragmentation channel allows fatty acyl composition determination, viz. the number of carbons and degrees of unsaturation, while neutral loss scan (NLS) of 368 Da renders sensitive detection and quantitation of CEs. The above ESI-MS/MS techniques, however, have a major limitation of not being able to provide carbon-carbon double bond (C=C) location information within fatty acyls of

CEs. Given that unsaturation in lipids play critical roles in their biochemical and biophysical properties, and many unsaturated fatty acids have multiple C=C location isomers fulfilling distinct biological roles, it is of great importance to characterize unsaturated CEs at the structural level of C=C locations [27–29].

The need to determine a specific lipid structure from coexisting isomers and isobars has drawn increasing awareness in the field of lipidomics [30, 31]. Some notable MS methods that are suitable for the analysis of different classes of lipids and provide C=C location information include charge-remote fragmentation induced by high energy CID [32], ozone-induced dissociation (OzID) [33–35], radical directed dissociation (RDD) [36, 37], helium metastable atom-activated dissociation (He-MAD) [38, 39], and electron impact excitation of ions from organics (EIEIO) [40, 41]. Recently, our group has demonstrated that the Patern-Büchi (PB) reaction [42], a photochemical reaction via the addition of electronically excited acetone to a C=C, can be applied to C=C location determination and location isomer quantitation for fatty acids and phospholipids when coupled with ESI-MS/MS [43–46]. In this study, we aim to expand the scope of the PB reaction to neutral lipids, such as CEs, which tend to have high composition of unsaturated fatty acyls. The factors that are key to this development have been identified, including proper solvent system that allows both good PB reaction yield and ionization for CE using ESI, and MS/MS methods that can allow confident structural determination and C=C location isomer quantitation. Commercially available CE standards were used for method development and optimization. The analytical capability of PB-MS/MS was further tested for analyzing CEs in human plasma.

## Experimental

### Nomenclature

Shorthand notation for CEs is taken from LIPID MAPS [47]. For example, CE 18:1(9Z) denotes a cholesteryl ester containing an 18-carbon fatty acyl chain. The numeral “1” after the carbon number refers to the degree of unsaturation of the fatty acyl. The location(s) of the C=C bond(s) is defined in  $\Delta^x$  nomenclature by counting from the alpha carbon of the fatty acyl and is indicated with the number(s) in parentheses. For polyunsaturated fatty acyl chains, the  $\omega$ -nomenclature is also used for simplicity in which the location of the first C=C is counted from the methyl end of the fatty acyl chain. Cis- or trans-configuration of C=C bond is denoted with Z and E nomenclature, respectively. For CE analysis from biological extract, the Z/E stereo-configurations are not assigned.

### Materials

CE standards, including CE 18:1 (9Z), CE 18:1 (11Z), CE 18:2 (9Z, 12Z), CE 18:3 (9Z, 12Z, 15Z), CE 18:3 (6Z, 9Z, 12Z), CE 20:4 (5Z, 8Z, 11Z, 14Z), and CE 22:5 (7Z, 10Z, 13Z, 16Z, 19Z), and lithium hydroxide (LiOH) were purchased from

Sigma-Aldrich (St. Louis, MO USA). Pooled normal human plasma with anticoagulant lithium heparin was obtained from Innovative Research, Inc. (Novi, MI, USA). Organic solvents were all LC grade and ultrapure water was obtained from a purification system at 0.03  $\mu\text{S cm}$ . CEs were extracted from 20  $\mu\text{L}$  of plasma following methyl-*tert*-butyl ether (MTBE) method with an extraction efficiency of  $71.0\% \pm 0.6\%$  obtained (from three replicates) [48].

### *PB-MS/MS for CE Analysis*

All samples were analyzed in positive ion mode using a 4000 QTRAP mass spectrometer (Sciex, Toronto, ON, CA) equipped with a home-built nanoESI source and a low pressure mercury lamp (primary emission at 254 nm; BHK Inc., Ontario, CA). CE standards (0.1–10  $\mu\text{M}$ ) were dissolved in acetone/methanol/dichloromethane/water = 40/30/20/10 (volume ratios) containing 100  $\mu\text{M}$  LiOH. The PB reaction was facilitated by UV irradiation of a pulled borosilicate glass capillary nanoESI tip, which contained a solution of CE. A scheme of the reaction setup is shown in Supporting Information (SI), Figure S1. Multiple modes of MS/MS, including neutral loss scan (NLS),  $\text{MS}^2$  via beam-type CID, and  $\text{MS}^3$  via sequential beam-type CID and on-resonance ion trap CID were employed in CE analysis. For NLS, collision energy (CE) was optimized at 40 eV. In beam-type CID, the precursor ions were isolated by Q1 and accelerated to q2 for collisional activation with collision energy defined by the DC potential difference between Q0 and q2, which was typically within the range 35–40 V. Ion trap CID was carried out in Q3 linear ion trap, where a dipolar excitation was used for on-resonance collisional activation. The activation amplitudes were within the range 40–50 mV for 200 ms. The characteristic parameters of the mass spectrometer during this study were set as follows: spray voltage, 1200–1500 V; curtain gas, 10 psi; and declustering potential, 180 V. Data acquisition, processing, and instrument control were performed using Analyst 1.5 software.

## Results and Discussions

### *Online Coupling of the PB Reaction and NanoESI-MS for CE Analysis*

A simple binary mixture of acetone/water solvent system has been used for the analysis of fatty acids and phospholipids with acetone serving as both the PB reaction reagent and co-solvent in subsequent online ESI-MS or nanoESI-MS [43, 45]. This condition works well for both PB reaction and ionization since the above two classes of lipids have reasonable solubility in such polar solvent system. It is worth noting that organic solvent other than acetone is minimized in the solvent system to reduce possible side reactions involving radical intermediates formed from Norrish Type I cleavage of acetone [45]. CEs have very limited solubility in water and they are typically dissolved in methanol/chloroform (4:1 volume ratio) for ESI-MS analysis [23, 25]. Consequently, acetone/water solvent

system developed for polar lipids cannot be directly applied for the PB reaction and nanoESI-MS of CEs. Our first task was targeted to developing a solvent system that could provide good PB reaction of CE. Pure acetone was evaluated as the solvent for a model CE compound, CE 18:1(9Z) (5  $\mu\text{M}$ ), for various lengths of reaction time (10 s to 3 min) before reconstituting in methanol/chloroform (4:1 volume ratio, 100  $\mu\text{M}$  LiOH) for nanoESI. The PB reaction yield was found low and was accompanied by a large extent of side reactions. It was hypothesized that because of the nonpolar nature of CE molecules, the fatty acyls might prefer strong interactions with their own cholesteryl moieties and therefore have reduced interactions with the more polar acetone solvent molecules. We suspected that the addition of less polar organic solvent into acetone might be necessary to enhance effective interaction between acetone and CE fatty acyls. A series of organic solvents (10%–50% volume ratio relative to acetone) including chloroform ( $\text{CHCl}_3$ ), dichloromethane ( $\text{CH}_2\text{Cl}_2$ ), and hexane were examined. Dichloromethane was found as the best solvent to provide reasonable reaction yield and limited degree of side reactions among all organic solvents tested. An example of reaction spectrum involving  $\text{CHCl}_3$  as a co-solvent is shown in SI, Figure S2, which suffers from a high degree of CE ion signal loss and limited formation of the PB products.

The binary mixture of acetone/dichloromethane, however, was not miscible with even 10% of aqueous solution of salts, i.e., LiOH, the addition of which was necessary to enhance CE adduct ion formation and detection in ESI. Upon various tests, we found that methanol could be added as a co-solvent leading to a homogenous solution and ensuring stable ionization during nanoESI. The commonly used adduct ions for ESI analysis of CE, including lithium ( $\text{Li}^+$ ), ammonium ( $\text{NH}_4^+$ ), and sodium ( $\text{Na}^+$ ) were evaluated for their compatibility with PB-MS/MS.  $\text{Li}^+$  adduct of CE had combined advantages of relatively high ionization efficiency (relative to  $\text{Na}^+$  adduct) and forming abundant fatty acyl fragment ion (relative to  $\text{NH}_4^+$  adduct) under CID, and was used for further studies. After optimizations, a solvent system composed of acetone/methanol/dichloromethane/water (40/30/20/10) and 100  $\mu\text{M}$  LiOH was identified as the best solvent condition for conducting online PB-nanoESI-MS for CE analysis.

Data in Figure 2 show typical mass spectra of CE 18:1(9Z) before and after the PB reaction using such a solvent system. Before reaction (Figure 2a), only intact CE at  $m/z$  657.4 ( $[\text{CE} + \text{Li}]^+$ ) was observed as the dominant species. The peak at  $m/z$  673.4 is oxidized CE 18:1 (oxidation likely at the cholesteryl ring), existed in the original sample received. The PB reaction became stable after 1.5 min UV irradiation and the PB products, consisting of two structural isomers (structures shown in the inset of Figure 2), were detected at  $m/z$  715.6 ( $[\text{CE} - \text{PB} + \text{Li}]^+$ ) (Figure 2b). The PB products have a characteristic mass increase of 58 Da from intact CE due to acetone addition to a C=C bond. Under such reaction condition, the PB reaction was achieved with 20%–30% yield. A small degree of side reaction was observed at  $m/z$  687.5, showing a mass increase of 30 Da from intact CE 18:1 ions. When  $\text{CD}_3\text{OH}$  was used in the

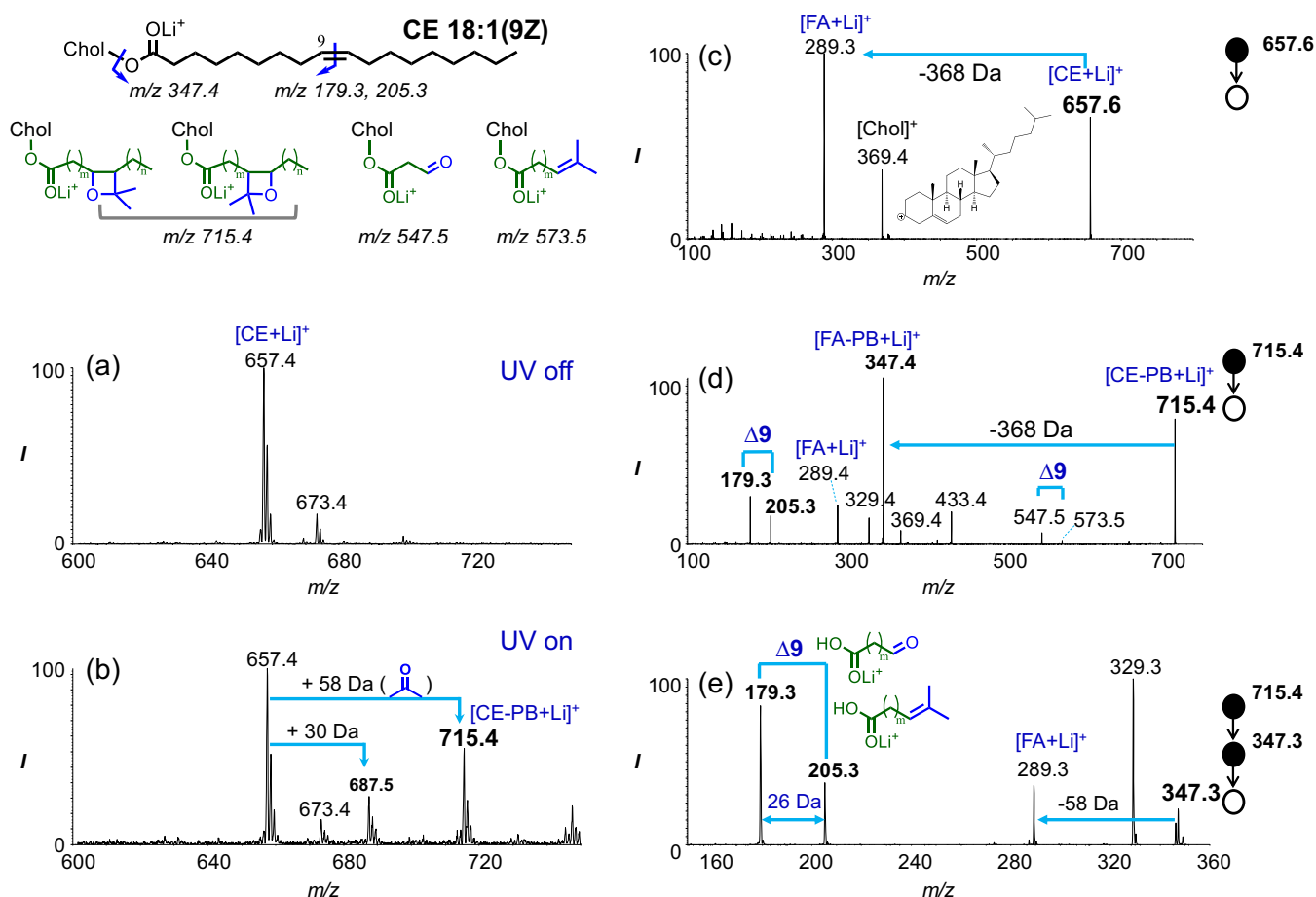


**Figure 2.** PB -MS/MS of CE 18:1 (9Z) 5  $\mu\text{M}$  in acetone/methanol/dichloromethane/water (40/30/20/10) containing 100  $\mu\text{M}$  LiOH. NanoESI MS<sup>1</sup> spectra in positive ion mode: (a) before reaction and (b) after the PB reaction. MS<sup>2</sup> beam-type CID of (c) intact CE ions ([CE+Li]<sup>+</sup>) at  $m/z$  657.6 and (d) the PB product ([CE - PB + Li]<sup>+</sup>) at  $m/z$  715.4. (e) MS<sup>3</sup> ion trap CID of [FA + 58 + Li]<sup>+</sup> ( $m/z$  347.3)

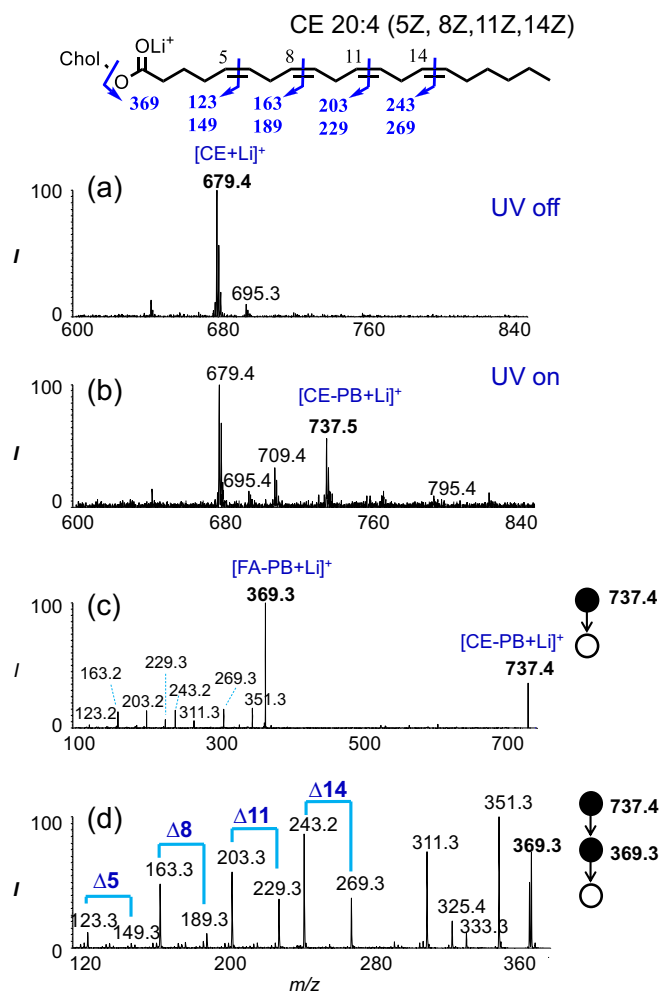
reaction, this side reaction product was detected at  $m/z$  689.5. The 2 Da mass shift suggests that hydroxyl methyl radical ( $\bullet\text{CH}_2\text{OH}$ ) is formed and added to CE (likely to a C=C). This process might involve the formation of Norrish Type I products of acetone, such as methyl radical ( $\bullet\text{CH}_3$ ) and acetyl radical ( $\text{CH}_3(\text{O})\text{C}\bullet$ ), which is concomitant under the PB reaction condition [49]. These radical intermediates further react with methanol and form hydroxyl methyl radical via hydrogen abstraction. Hydroxyl methyl radical adds on to a C=C bond; upon loss of a hydrogen atom, the hydroxyl methyl modified product is formed, having a mass 30 Da higher than the intact CE molecule.

Figure 2c and d compare MS<sup>2</sup> CID of intact CE 18:1(9Z) lithium adduct ([CE + Li]<sup>+</sup>) versus its PB reaction product ([CE - PB + Li]<sup>+</sup>). Intact CE ions ( $m/z$  657.6) produce two complementary fragment ions: lithiated fatty acyl ion ([FA + Li]<sup>+</sup>) at  $m/z$  289.4 and cholestene cation ([Chol]<sup>+</sup>) at  $m/z$  369.4. These two characteristic fragment ions are also detected, however, with significantly reduced relative intensities in MS<sup>2</sup> CID of the PB reaction products (Figure 2d). Instead, ions at  $m/z$  347.4 corresponding to acetone addition to the fatty acyl chain ([FA - PB + Li]<sup>+</sup>) is the most abundant fragment peak. Interestingly, the fragment containing acetone addition to cholesterol ring

( $m/z$  433.4) is detected at 20% intensity relative to [FA - PB + Li]<sup>+</sup> peak. It is worth noting that CE 18:1(9Z) consists of one C=C bond within the cholesteryl ring and one in its fatty acyl chain. The above results suggest that the PB reaction is preferred at a C=C with less steric hindrance. Two pairs of fragments related to the location of C=C in fatty acyl are also detected: ions at  $m/z$  547.5 and 573.5 and ions at  $m/z$  179.3 and 205.3 (structures shown in the inset of Figure 2). The characteristic 26 Da mass difference within each pair of ions clearly suggests that they each result from rupture of the four-membered oxatane rings of the two PB products formed. The former pair consists of intact cholesteryl moiety, whereas the latter pair are likely produced from sequential fragmentation of [FA - PB + Li]<sup>+</sup> ions. Indeed, MS<sup>3</sup> CID of [FA - PB + Li]<sup>+</sup> ( $m/z$  347.4, Figure 2e) leads to abundant formation of ions at  $m/z$  179.3 and 205.3. Although the location of C=C in fatty acyl chain can be readily deduced from MS<sup>2</sup> CID as shown in Figure 2d, these C=C diagnostics are much more dominant in MS<sup>3</sup> CID, which is later found to be useful in mixture analysis.

Acetone/methanol/dichloromethane/water (40/30/20/10) solvent system was also applied to standard CEs containing multiple C=C bonds to test its performance for the PB reaction. Figure 3a and b compare nanoESI-MS spectra of





**Figure 3.** PB-MS/MS of CE 20:4 (5Z, 8Z, 11Z, 14Z). NanoESI MS<sup>1</sup> spectra in positive ion mode: (a) before reaction and (b) after the PB reaction. (c) MS<sup>2</sup> beam-type CID of the PB reaction product ([CE-PB + Li]<sup>+</sup>) at *m/z* 737.4, (d) MS<sup>3</sup> ion trap CID of [FA-PB + Li]<sup>+</sup> (*m/z* 369.3) The fragmentation map of CE 20:4 is shown as an inset in Figure 3

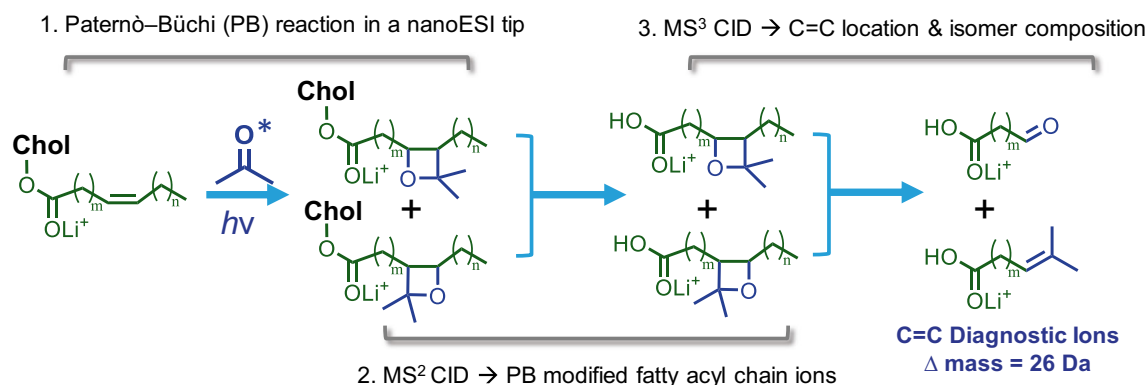
5 μM CE 20:4 (5Z, 8Z, 11Z, 14Z) before and after the PB reaction. The single acetone addition product ([CE-PB + Li]<sup>+</sup>, *m/z* 737.5) is the most abundant product peak after the PB reaction with very limited sequential acetone addition product, i.e., peak at *m/z* 795.4 observed (Figure 3b). Previous studies on the PB reactions of fatty acids and phospholipids suggest that the formation of single acetone addition PB product is most desirable in terms of generating easy-to-interpret C=C diagnostic ions for structural analysis. Ethanol at 10%–40% volume% has been added to acetone/water reaction solvent to suppress sequential PB reaction product formation for polyunsaturated fatty acyls, which have faster reactions than mono-unsaturated fatty acyls [46]. Since 30% of methanol is already used in the solvent system for CE analysis, it explains why single acetone addition product is the most abundant product. Unfortunately, a side reaction due to hydroxyl methyl radical addition to C=C bond, such as the peak at *m/z* 709 in Figure 3b is also formed.

Figure 3c shows MS<sup>2</sup> beam-type CID of [CE-PB + Li]<sup>+</sup> ions at *m/z* 737.4, the single acetone addition PB product of CE 20:4. [FA + 58 + Li]<sup>+</sup> (*m/z* 369.3) is the most abundant fragment peak, consistent with that observed from PB-MS/MS of CE 18:1. Due to sequential fragmentation of [FA-PB + Li]<sup>+</sup>, C=C diagnostic ions corresponding to the four C=C bonds in the fatty acyl chain are also present in the MS<sup>2</sup> CID spectrum, however, with relatively low ion intensities. These C=C diagnostic ions (*m/z* 123/149, 163/189, 203/229, 243/269) are more prominent in MS<sup>3</sup> ion trap CID (Figure 3d), leading to unambiguous assignment of C=C bond locations at Δ5, 8, 11, and 14, respectively (fragmentation map shown in the inset of Figure 3).

### PB-MS<sup>3</sup> CID for CE C=C Location Isomer Analysis

Many unsaturated lipids coexist with one or multiple C=C location isomers in their biological environments and fulfill distinct functions [28, 50, 51]. Our previous studies demonstrate that PB-MS/MS can be readily coupled with shotgun lipid analysis and provide C=C location information as well as C=C location isomer composition information without prior separation [44]. The key step in these experiments is to generate distinct C=C diagnostic ions in PB-MS/MS. Their *m/z* information leads to C=C location determination, whereas the relative ion intensities of the diagnostic ions provide quantitative information. The earlier experiments on CE standards show that MS<sup>3</sup> CID of the PB reaction modified fatty acyl chain ions ([FA-PB + Li]<sup>+</sup>) provides stronger C=C diagnostic ion signals together with easy-to-interpret spectrum compared with MS<sup>2</sup> CID of the PB reaction product ([CE-PB + Li]<sup>+</sup>). Therefore, a PB-MS<sup>3</sup> CID approach outlined in Scheme 1 was further tested for C=C location isomer analysis of unsaturated CEs.

Figure 4a demonstrates PB-MS<sup>3</sup> CID of [FA-PB + Li]<sup>+</sup> (*m/z* 347) derived from an equal molar mixture of CE 18:1 (9Z) and CE 18:1 (11Z) at total concentration of 10 μM. Their corresponding C=C diagnostic ions, viz. *m/z* 179/205 for Δ9 isomer and *m/z* 207/233 for Δ11 isomer are formed abundantly in the MS<sup>3</sup> spectrum, allowing confident determination of C=C location for each isomer. In order to obtain rigorous quantitative information, a series of mixtures of CE 18:1(9Z) and CE18:1 (11Z) with total concentration kept at 10 μM but varying molar ratios was prepared and subjected to PB-MS<sup>3</sup> CID. Peak areas of the two C=C diagnostic ions of each isomer were summed and their ratios were plotted against molar ratios (Figure 4b). Good linearity ( $R^2 = 0.992$ ) was obtained in a wide dynamic range (molar ratios from 15:1 to 1:15) for such a calibration curve. We then evaluated PB-MS<sup>3</sup> for quantitative analysis of mixtures containing two common CE 18:3 isomers: ω-6 (C=C at 6Z, 9Z, 12Z) and ω-3(C=C at 9Z, 12Z, 15Z). Figure 4c shows MS<sup>3</sup> CID of [FA-PB + Li]<sup>+</sup> ions resulting from single acetone addition to CE 18:3 with the ω-6 and ω-3 isomers each at 5 μM. Because each isomer contains three C=C bonds, six pairs of C=C diagnostic ions are produced in the range *m/z* 130–260 (fragmentation maps for both isomers



**Scheme 1.** A PB-MS<sup>3</sup> CID strategy for the determination of C=C location in fatty acyl chains of CEs and their C=C location isomer quantitation

shown in Figure 4d). The peak areas of the three pairs of C=C diagnostic ions derived from each isomer were summed up and used for quantitation in the same fashion as described for CE 18:1 isomer analysis. The calibration curve showed good linearity and dynamic range. We also tried simplifying this process by only using one C=C diagnostic peak from each isomer. In fact, calibration curves with good linearity were obtained from choosing different combinations of C=C diagnostic ions. Figure 4e demonstrates an example of such a calibration curve based on plotting peak area ratios of  $m/z$  137 of  $\omega$ -6 isomer to  $m/z$  259 of  $\omega$ -3 isomer against molar ratios of  $\omega$ -6 versus  $\omega$ -3. Again, good linearity is achieved in a wide dynamic range (molar ratio from 1:15 to 15:1). These two peaks were found to suffer the least interference from chemical noises in the analysis of CEs from human plasma and, therefore, they were chosen for isomer quantitation. The experiments on standard CEs and CE C=C location isomers clearly support that the PB-MS<sup>3</sup> CID approach is successful in providing C=C location information and achieving relative quantitation for C=C location isomers if they coexist. This method is then further applied to CE extracts from human plasma to test its analytical utility in mixture analysis.

### Analysis CE Extract from Human Plasma

CEs are relatively abundant species in human plasma and quantitative analyses of CE species in human plasma have been reported using either shotgun or LC-MS methods; the C=C double bond location isomer identification and relative composition have not been determined [7]. We are interested in providing C=C location information for unsaturated CE species, especially detecting coexisting C=C location isomers in human plasma by applying PB-MS<sup>3</sup> CID approach (Scheme 1) in the context of shotgun lipid analysis. CEs were extracted from human plasma (20  $\mu$ L) based on the MTBE method and an extraction efficiency of  $71.0\% \pm 0.6\%$  was achieved, comparable to literature report [48]. The extract was dried and reconstituted into 1 mL acetone/methanol/dichloromethane/water (40/30/20/10) containing 100  $\mu$ M LiOH for nanoESI-MS analysis.

Figure 5a shows the CE profile obtained via NLS of 368 Da (cholesteryl, C<sub>27</sub>H<sub>44</sub>) before applying the PB reaction. Consistent with literature report, CE 18:2 ( $m/z$  655.7) is the most abundant species, followed by CE 18:1 ( $m/z$  657.8) and CE 20:4 ( $m/z$  679.8), whereas CE 16:1 ( $m/z$  629.6), CE 16:0 ( $m/z$  631.8),

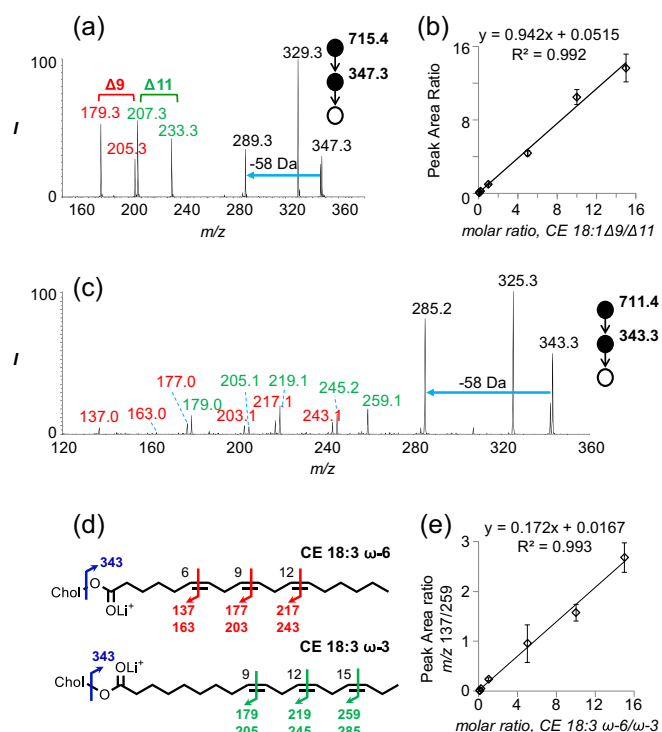


**Figure 4.** A PB-MS<sup>3</sup> CID approach to identify and quantify CE C=C location isomers. **(a)** PB-MS<sup>3</sup> CID of  $m/z$  347.3 from the PB reaction product of 1/1 molar ratio of CE 18:1 (9Z)/(11Z) at a total concentration of 10  $\mu$ M. **(b)** Linear relationship established from plotting C=C diagnostic ion peak area ratio and molar ratio of CE 18:1 C=C location isomers. **(c)** PB-MS<sup>3</sup> CID of  $m/z$  343.3 from PB reaction product of 1/1 molar ratio of CE 18:3 (6Z, 9Z, 12Z) ( $\omega$ -6)/(9Z, 12Z, 15Z) ( $\omega$ -3) at a total concentration of 10  $\mu$ M. **(d)** Fragmentation maps of CE 18:3  $\omega$ -6 and  $\omega$ -3 isomers. **(e)** Linear relationship established from plotting peak area ratios of  $m/z$  137/259 against molar ratios of CE 18:3 isomers

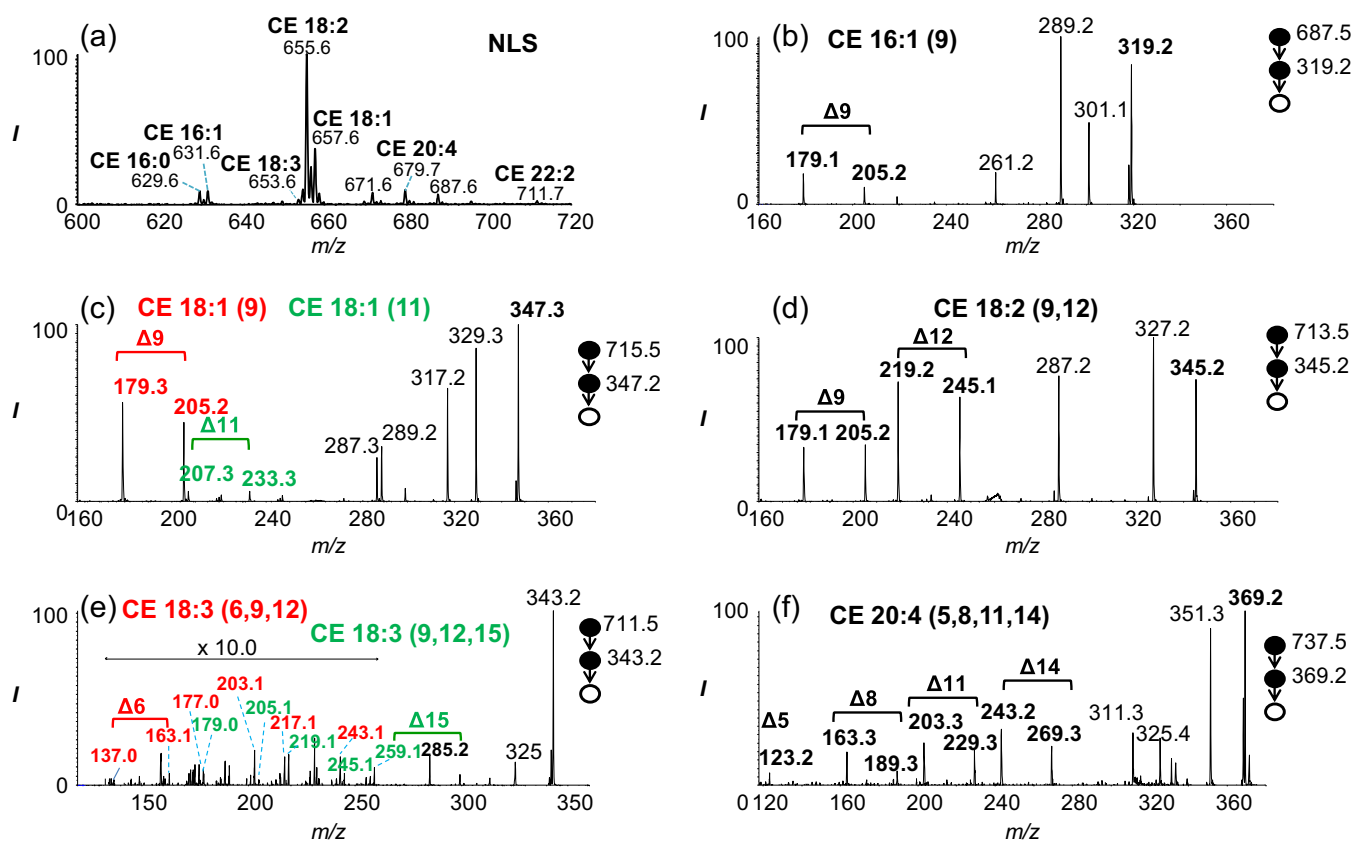


**Figure 5.** Identification of major unsaturated CE species from human plasma using PB-MS/MS. **(a)** Profile of CEs from human plasma based on NLS of 368 Da (cholesterene,  $C_{27}H_{44}$ ). PB-MS<sup>3</sup> CID of  $[FA-PB+Li]^+$  ions of **(b)** CE 16:1, **(c)** CE 18:1, **(d)** CE 18:2, **(e)** CE 18:3, and **(f)** CE 20:4

and CE 18:3 ( $m/z$  653.8) are detected as less abundant species [7]. Unsaturated CE species were further subjected to PB-MS<sup>3</sup> CID for C=C location determination. Corresponding PB-MS<sup>3</sup> CID data are shown Figure 5b–f with C=C diagnostic ions labeled in each spectrum. Fragmentation maps of all identified unsaturated CEs are listed in SI, Figure S3. Due to fast cis-trans isomerization of C=C under PB reaction conditions [42], the stereo-configurations of C=C cannot be determined from PB-MS/MS; therefore, only the locations of C=C within CE fatty acyls are reported here. Among them, CE 16:1(9), CE 18:2 (9, 12), and CE 20:4 (5, 8, 11, 14) existed as pure compounds. For CE 18:1,  $\Delta 9$  and  $\Delta 11$  isomers were both detected and their molar ratio was determined to be 12/1 based on the calibration curve shown in Figure 4b. CE 18:3 is a relatively low concentration species, only accounting for 2% relative intensity of CE 18:2 (Figure 5a). Given the capability of performing MS<sup>3</sup> CID, diagnostic ions of the two isomers of CE 18:3:  $\omega$ -6 (C=C at  $\Delta 6, 9, 12$ ) and  $\omega$ -3 (C=C at  $\Delta 9, 12, 15$ ) are still detected (Figure 5f). The presence of C=C diagnostic ions in pairs with a signature separation of 26 Da greatly enhances the level of confidence in C=C location identification even though they have relatively low signal-to-noise ratios (S/N). For isomeric composition determination, C=C diagnostic peaks at  $m/z$  259 of CE 18:3  $\omega$ -6 isomer and  $m/z$  137 of the  $\omega$ -3 isomers were chosen for relative quantitation because these ions experienced the least interference from chemical noises.

Using the calibration curve established in Figure 4e, we successfully determined molar ratio of  $\omega$ -6/ $\omega$ -3 isomers to be 3/5.

Use of internal standard (IS) helps to correct for errors associated with nanoESI spray instability, matrix effect, loss of analyte during sample preparation, and CID conditions. An appropriate IS should have similar physical property and ionization efficiency as CE analytes. In this study, CE 22:5 (7Z, 10Z, 13Z, 16Z, 19Z), which was not detected in human plasma, was chosen to be the internal IS. A fixed amount of IS (2  $\mu$ M) was added into solutions containing different concentrations of reference standards (RS). Then a neutral loss scan (NLS) of 368 Da (cholesterene,  $C_{27}H_{44}$ ) was used for quantitation of different CE species. The calibration curves for CE 16:1 (9Z), CE 18:1(9Z), CE 18:2 (9Z, 12Z), CE 18:3 (9Z, 12Z, 15Z), and CE 20:4 (5Z, 8Z, 11Z, 14Z) are shown in SI, Figure S4. Good linear relationship was obtained and the limit of quantitation (LOQ) was 0.1  $\mu$ M achieved for all CE species. For pure unsaturated CEs, viz. CE 16:1, CE 18:2, CE 20:4, their concentrations were directly obtained based on NLS and established calibration curves. For CE species containing C=C location isomers, such as CE 18:1 and CE 18:3, the sum concentrations were determined from NLS and then each isomer's concentration was calculated using its composition ratio obtained from PB-MS<sup>3</sup> experiments. Table 1 summarizes quantitative information of the above five unsaturated CEs

**Table 1.** Quantitative Analysis of Major Unsaturated CE Species in Human Plasma

Unsaturated CE	Concentration ( $\mu\text{M}$ )	MW Da	[M + Li] <sup>+</sup> m/z
CE 16:1 (9)	98 ± 13	622.6	629.6
CE 18:1 (total)	414 ± 48		
CE 18:1 (9)	382 ± 44	650.6	657.6
CE 18:1 (11)	32 ± 4		
CE 18:2 (9, 12)	(1.30 ± 0.11) × 10 <sup>3</sup>	648.6	655.6
CE 18:3 (total)	24.0 ± 1.6		
CE 18:3 (6, 9, 12)/ $\omega$ -6	9.0 ± 0.6	646.6	653.6
CE 18:3 (9, 12, 15)/ $\omega$ -3	15.0 ± 1.0		
CE 20:4 (5, 8, 11, 14)	127 ± 4	672.6	679.6

\* Ionic species detected in NLS (368 Da) for CE quantitation.

from human plasma. It is worth pointing out that the identification and quantitation of CE 18:1 and CE 18:3 isomers are reported for the first time without prior separations. Moreover, the capability of performing quantitative analysis on C=C location isomers of relatively low abundance CEs, such as CE 18:3, is enabled by high specificity and sensitivity innate in the PB-MS<sup>3</sup> CID approach.

Free FAs of the same human plasma sample were analyzed by PB-MS/MS and reported previously [46]. Comparing to CE data collected from this study, we notice that the C=C locations within fatty acyls are conserved no matter if they are in free FAs or in more complicated lipid molecules, such as CEs. For instance, CE 18:2 is a pure form with C=C located at  $\Delta$ 9 and  $\Delta$ 12, and the same is detected for FA 18:2. CE 18:1 has  $\Delta$ 9 and  $\Delta$ 11, two location isomers, and their molar ratio (12/1) is very close to that of free FA 18:1 ( $\Delta$ 9/ $\Delta$ 11 = 11/1). Similarly, the same  $\omega$ -6 and  $\omega$ -3 isomers of FA 18:3 are detected for CE 18:3. The conservation of fatty acyl identities in different classes of lipids reflects them being common building blocks in lipid biosynthesis. More importantly, this type of information could be used as a guide for the identification of unsaturated lipids of different classes.

## Conclusions

In this study, an approach based on PB-MS<sup>3</sup> CID has been developed for the analysis of CEs containing unsaturated fatty acyl chains from mixtures. An important step of the development is to determine a proper solvent system that allows for both good PB reaction and ionization via nanoESI. Since CE is nonpolar, adding a nonpolar co-solvent, such as CH<sub>2</sub>Cl<sub>2</sub> (20%), to acetone (40%) is necessary for achieving good yields in the PB reactions, while adding another relatively polar co-solvent, MeOH (30%) helps in forming homogenous solution and maintaining stable nanoESI upon the addition of 10% of LiOH aqueous solution. The PB products of CEs in the form of lithium adduct ions ([CE - PB + Li]<sup>+</sup>) can be detected abundantly after reaction. Collisional activation of [CE - PB + Li]<sup>+</sup> results in prominent formation of PB modified fatty acyl ions ([FA - PB + Li]<sup>+</sup>), while MS<sup>3</sup> CID of [FA - PB + Li]<sup>+</sup> leads to C=C diagnostic ion formation, which are

employed in the determination of C=C location and of C=C location isomer composition. The analytical utility of PB-MS<sup>3</sup> CID was demonstrated with CE analysis from human plasma. A series of CEs containing unsaturated fatty acyl chains was identified and quantified at structural level of the C=C locations, unveiling several coexisting C=C location isomers of CEs. Such detailed information is generally not obtainable using conventional lipid analysis methods. Overall, the PB-MS<sup>3</sup> CID approach is simple, fast, and compatible with shotgun lipid analysis workflow. It also offers a distinct advantage of high molecular specificity due to coupling C=C site specific derivatization and MS<sup>3</sup>. These advantages would be especially attractive for discovering composition changes of CE C=C location isomers related to diseases or physiological changes. Undesirable aspects associated with the current method include low PB reaction yield and unwanted side reactions due to the use of MeOH as a co-solvent, both of which limit sensitivity of the PB-MS<sup>3</sup> CID approach. Future studies will focus on developing an improved reaction system for CE and other non-polar lipids.

## Acknowledgements

Financial support from NSF CHE-1308114 and NIH R01GM118484 is greatly appreciated. X.Y. acknowledges ASMS research award for supporting the research on radical ion chemistry.

## References

- Horton, J.D., Goldstein, J.L., Brown, M.S.: Srebps: Activators of the complete program of cholesterol and fatty acid synthesis in the liver. *J. Clin. Invest.* **109**, 1125–1131 (2002)
- Brown, M.S., Ho, Y.K., Goldstein, J.L.: The cholesteryl ester cycle in macrophage foam cells. Continual hydrolysis and re-esterification of cytoplasmic cholesteryl esters. *J. Biol. Chem.* **255**, 9344–9352 (1980)
- Schwartz, C.C., VandenBroek, J.M., Cooper, P.S.: Lipoprotein cholesteryl ester production, transfer, and output in vivo in humans. *J. Lipid Res.* **45**, 1594–1607 (2004)
- Suckling, K.E., Stange, E.F.: Role of Acyl-CoA: cholesterol acyltransferase in cellular cholesterol metabolism. *J. Lipid Res.* **26**, 647–671 (1985)



5. Yang, H., Bard, M., Bruner, D.A., Gleeson, A., Deckelbaum, R.J., Aljinovic, G., Pohl, T.M., Rothstein, R., Sturley, S.L.: Sterol esterification in yeast: a two-gene process. *Science* **272**, 1353–1356 (1996)
6. Francone, O.L., Gurakar, A., Fielding, C.: Distribution and functions of lecithin: cholesterol acyltransferase and cholesteryl ester transfer protein in plasma lipoproteins. Evidence for a functional unit containing these activities together with apolipoproteins *a-i* and *d* that catalyzes the esterification and transfer of cell-derived cholesterol. *J. Biol. Chem.* **264**, 7066–7072 (1989)
7. Quehenberger, O., Armando, A.M., Brown, A.H., Milne, S.B., Myers, D.S., Merrill, A.H., Bandyopadhyay, S., Jones, K.N., Kelly, S., Shaner, R.L., Sullards, C.M., Wang, E., Murphy, R.C., Barkley, R.M., Leiker, T.J., Raetz, C.R.H., Guan, Z., Laird, G.M., Six, D.A., Russell, D.W., McDonald, J.G., Subramaniam, S., Fahy, E., Dennis, E.A.: Lipidomics reveals a remarkable diversity of lipids in human plasma. *J. Lipid Res.* **51**, 3299–3305 (2010)
8. Nishikawa, Y., Quittnat, F., Stedman, T.T., Voelker, D.R., Choi, J.-Y., Zahn, M., Yang, M., Pypaert, M., Joiner, K.A., Coppens, I.: Host cell lipids control cholesteryl ester synthesis and storage in intracellular toxoplasma. *Cell. Microbiol.* **7**, 849–867 (2005)
9. Lee, R.G., Kelley, K.L., Sawyer, J.K., Farese, R.V., Parks, J.S., Rudel, L.L.: Plasma cholesteryl esters provided by lecithin:Cholesterol acyltransferase and acyl-coenzyme A: cholesterol acyltransferase 2 have opposite atherosclerotic potential. *Circ. Res.* **95**, 998–1004 (2004)
10. Crowe, F.L., Skeaff, C.M., Green, T.J., Gray, A.R.: Serum fatty acids as biomarkers of fat intake predict serum cholesterol concentrations in a population-based survey of New Zealand adolescents and adults. *Am. J. Clin. Nutr.* **83**, 887–894 (2006)
11. Harkewicz, R., Hartvigsen, K., Almazan, F., Dennis, E.A., Witztum, J.L., Miller, Y.I.: Cholesteryl ester hydroperoxides are biologically active components of minimally oxidized LDL. *J. Biol. Chem.* **283**, 10241–10251 (2008)
12. Yue, S., Li, J., Lee, S.-Y., Lee, H.J., Shao, T., Song, B., Cheng, L., Masterson, T.A., Liu, X., Ratliff, T.L., Cheng, J.-X.: Cholesteryl ester accumulation induced by PTEN loss and pi3k/akt activation underlies human prostate cancer aggressiveness. *Cell Metab.* **19**, 393–406 (2014)
13. Peck, B., Schulze, A.: Cholesteryl esters: fueling the fury of prostate cancer. *Cell Metab.* **19**, 350–352 (2014)
14. German, J.B., Gillies, L.A., Smilowitz, J.T., Zivkovic, A.M., Watkins, S.M.: Lipidomics and lipid profiling in metabolomics. *Curr. Opin. Lipid.* **18**, 66–71 (2007)
15. Shevchenko, A., Simons, K.: Lipidomics: coming to grips with lipid diversity. *Nat. Rev. Mol. Cell Biol.* **11**, 593–598 (2010)
16. Murphy, R.C., Fiedler, J., Hevko, J.: Analysis of nonvolatile lipids by mass spectrometry. *Chem. Rev.* **101**, 479–526 (2001)
17. Fenn, J., Mann, M., Meng, C., Wong, S., Whitehouse, C.: Electrospray ionization for mass spectrometry of large biomolecules. *Science* **246**, 64–71 (1989)
18. Han, X., Gross, R.W.: Electrospray ionization mass spectroscopic analysis of human erythrocyte plasma membrane phospholipids. *Proc. Natl. Acad. Sci. U. S. A.* **91**, 10635–10639 (1994)
19. Han, X.L., Gross, R.W.: Global analyses of cellular lipidomes directly from crude extracts of biological samples by esi mass spectrometry: a bridge to lipidomics. *J. Lipid Res.* **44**, 1071–1079 (2003)
20. Han, X.L., Gross, R.W.: Shotgun lipidomics: Electrospray ionization mass spectrometric analysis and quantitation of cellular lipidomes directly from crude extracts of biological samples. *Mass Spectrom. Rev.* **24**, 367–412 (2005)
21. Bird, S.S., Marur, V.R., Sniatynski, M.J., Greenberg, H.K., Kristal, B.S.: Lipidomics profiling by high-resolution LC-MS and high-energy collisional dissociation fragmentation: focus on characterization of mitochondrial cardiolipins and monolysocardiolipins. *Anal. Chem.* **83**, 940–949 (2010)
22. Nygren, H., Seppänen-Laakso, T., Castillo, S., Hyötyläinen, T., Orešič, M.: Liquid chromatography-mass spectrometry (LC-MS)-based lipidomics for studies of body fluids and tissues. Springer (2011)
23. Murphy, R.C., Leiker, T.J., Barkley, R.M.: Glycerolipid and cholesterol ester analyses in biological samples by mass spectrometry. *Biochim. Biophys. Acta Mol. Cell Biol. Lipids* **1811**, 776–783 (2011)
24. Murphy, R.C.: Tandem mass spectrometry of lipids: molecular analysis of complex lipids. *Royal Soc. Chem.* (2014)
25. Bowden, J.A., Albert, C.J., Barnaby, O.S., Ford, D.A.: Analysis of cholesteryl esters and diacylglycerols using lithiated adducts and electrospray ionization-tandem mass spectrometry. *Anal. Biochem.* **417**, 202–210 (2011)
26. Bowden, J.A., Shao, F., Albert, C.J., Lally, J.W., Brown, R.J., Procknow, J.D., Stephenson, A.H., Ford, D.A.: Electrospray ionization tandem mass spectrometry of sodiated adducts of cholesteryl esters. *Lipids* **46**, 1169–1179 (2011)
27. Martínez-Seara, H., Róg, T., Pasenkiewicz-Gierula, M., Vattulainen, I., Karttunen, M., Reigada, R.: Interplay of unsaturated phospholipids and cholesterol in membranes: effect of the double-bond position. *Biophys. J.* **95**, 3295–3305 (2008)
28. Johnson, D.W., Beckman, K., Fellenberg, A.J., Robinson, B.S., Poulos, A.: Monoenoic fatty acids in human brain lipids: isomer identification and distribution. *Lipids* **27**, 177–180 (1992)
29. Rustan, A.C., Drevon, C.A.: Fatty acids: Structures and properties. John Wiley and Sons (2005)
30. Hancock, S.E., Poad, B.L.J., Batarseh, A., Abbott, S.K., Mitchell, T.W.: Advances and unresolved challenges in the structural characterization of isomeric lipids. *Anal. Biochem.* (2016). doi:10.1016/j.ab.2016.1009.1014
31. Ryan, E., Reid, G.E.: Chemical derivatization and ultrahigh resolution and accurate mass spectrometry strategies for “shotgun” lipidome analysis. *Acc. Chem. Res.* **49**, 1596–1604 (2016)
32. Tomer, K.B., Crow, F.W., Gross, M.L.: Location of double-bond position in unsaturated fatty acids by negative ion MS/MS. *J. Am. Chem. Soc.* **105**, 5487–5488 (1983)
33. Thomas, M.C., Mitchell, T.W., Harman, D.G., Deeley, J.M., Nealon, J.R., Blanksby, S.J.: Ozone-induced dissociation: elucidation of double bond position within mass-selected lipid ions. *Anal. Chem.* **80**, 303–311 (2007)
34. Brown, S.H.J., Mitchell, T.W., Blanksby, S.J.: Analysis of unsaturated lipids by ozone-induced dissociation. *Biochim. Biophys. Acta Mol. Cell Biol. Lipids* **1811**, 807–817 (2011)
35. Pham, H.T., Maccarone, A.T., Thomas, M.C., Campbell, J.L., Mitchell, T.W., Blanksby, S.J.: Structural characterization of glycerophospholipids by combinations of ozone- and collision-induced dissociation mass spectrometry: the next step towards “top-down” lipidomics. *Analyst* **139**, 204–214 (2014)
36. Pham, H.T., Trevitt, A.J., Mitchell, T.W., Blanksby, S.J.: Rapid differentiation of isomeric lipids by photodissociation mass spectrometry of fatty acid derivatives. *Rapid Commun. Mass Spectrom.* **27**, 805–815 (2013)
37. Pham, H.T., Julian, R.R.: Radical delivery and fragmentation for structural analysis of glycerophospholipids. *Int. J. Mass Spectrom.* **370**, 58–65 (2014)
38. Deimler, R.E., Sander, M., Jackson, G.P.: Radical-induced fragmentation of phospholipid cations using metastable atom-activated dissociation mass spectrometry (MAD-MS). *Int. J. Mass Spectrom.* **390**, 178–186 (2015)
39. Li, P., Hoffmann, W.D., Jackson, G.P.: Multistage mass spectrometry of phospholipids using collision-induced dissociation (cid) and metastable atom-activated dissociation (MAD). *Int. J. Mass Spectrom.* **403**, 1–7 (2016)
40. Campbell, J.L., Baba, T.: Near-complete structural characterization of phosphatidylcholines using electron impact excitation of ions from organics. *Anal. Chem.* **87**, 5837–5845 (2015)
41. Baba, T., Campbell, J.L., Le Blanc, J.C.Y., Baker, P.R.S.: Structural identification of triacylglycerol isomers using electron impact excitation of ions from organics (EIEIO). *J. Lipid Res.* **57**, 2015–2027 (2016)
42. Büchi, G., Inman, C.G., Lipinsky, E.S.: Light-catalyzed organic reactions. I. The reaction of carbonyl compounds with 2-methyl-2-butene in the presence of ultraviolet light. *J. Am. Chem. Soc.* **76**, 4327–4331 (1954)
43. Ma, X., Xia, Y.: Pinpointing double bonds in lipids by Paternò-Büchi reactions and mass spectrometry. *Angew. Chem. Int. Ed.* **126**, 2592–2596 (2014)
44. Ma, X., Chong, L., Tian, R., Shi, R., Hu, T.Y., Ouyang, Z., Xia, Y.: Identification and quantitation of lipid C=C location isomers: A shotgun lipidomics approach enabled by photochemical reaction. *Proc. Natl. Acad. Sci. U. S. A.* **113**, 2573–2578 (2016)
45. Stinson, C.A., Xia, Y.: A method of coupling the Paternò-Büchi reaction with direct infusion esi-ms/ms for locating the C=C bond in glycerophospholipids. *Analyst* **141**, 3696–3704 (2016)
46. Ma, X., Zhao, X., Li, J., Zhang, W., Cheng, J.-X., Ouyang, Z., Xia, Y.: Photochemical tagging for quantification of unsaturated fatty acids by mass spectrometry. *Anal. Chem.* **88**, 8931–8935 (2016)

47. Liebisch, G., Vizcaíno, J.A., Köfeler, H., Trötz Müller, M., Griffiths, W.J., Schmitz, G., Spener, F., Wakelam, M.J.O.: Shorthand notation for lipid structures derived from mass spectrometry. *J. Lipid Res.* **54**, 1523–1530 (2013)
48. Matyash, V., Liebisch, G., Kurzchalia, T.V., Shevchenko, A., Schwudke, D.: Lipid extraction by methyl-tert-butyl ether for high-throughput lipidomics. *J. Lipid Res.* **49**, 1137–1146 (2008)
49. Norrish, R.G.W., Bramford, C.H.: Photodecomposition of aldehydes and ketones. *Nature* **138**, 1016 (1936)
50. Wijendran, V., Hayes, K.C.: Dietary *n*-6 and *n*-3 fatty acid balance and cardiovascular health. *Annu. Rev. Nutr.* **24**, 597–615 (2004)
51. Simopoulos, A.P.: The importance of the omega-6/omega-3 fatty acid ratio in cardiovascular disease and other chronic diseases. *Exp. Biol. Med.* **233**, 674–688 (2008)